

## Fermi surfaces and electronic topological transitions in metallic random alloys. II. $\text{Ag}_c\text{Pd}_{1-c}$

E. Bruno, B. Ginatempo, and E. S. Giuliano

*Dipartimento di Fisica, Università di Messina, Salita Sperone 31, 98166 Messina, Italy*

(Received 13 February 1995; revised manuscript received 26 May 1995)

We have calculated the Fermi surfaces of  $\text{Ag}_c\text{Pd}_{1-c}$  vs Ag atomic concentration, within the fully relativistic Korringa-Kohn-Rostoker-coherent-potential-approximation framework. The Fermi surfaces of these alloys change, on varying the concentration, from the Pd- to the Ag-like topology. This implies that a number of electronic topological transitions (ETT's) occur on changing the  $e/a$  ratio, as a consequence of the fact that the Fermi level moves away from the  $d$  states towards the  $sp$  states. It is well known that such changes in connectivity of the Fermi surfaces affect transport coefficients; however, as we have shown in Paper I, equilibrium properties such as equilibrium volume, specific heat, enthalpy of mixing, etc., also display anomalies at the same concentrations where such topological changes occur. In particular we have found 5 ETT's in correspondence to the deviations from Vegard's law of the lattice parameter shown in Paper I. Another unexpected result of this study is that, in the range of atomic concentration between 0.55 and 0.69, this alloy Fermi surface is simply connected, although nonspherical, as for a simple metal. Moreover, we show that a fully relativistic study is necessary for AgPd Fermi surfaces, because the spin-orbit interaction is responsible for the fact that the two hole pockets at  $X$  close at different concentrations.

### I. INTRODUCTION

The  $\text{Ag}_c\text{Pd}_{1-c}$  metallic alloy has deserved a lot of attention in the past, both from theoretical and experimental points of view.<sup>1-7</sup> The application of the coherent potential approximation (CPA) was, at first,<sup>2</sup> able to show its intrinsic "split-band" properties, adding value to CPA in comparison with the earliest virtual crystal and average  $T$ -matrix approximation. Later on, in 1982, it was one of the first systems where the self-consistent-field Korringa-Kohn-Rostoker (SCF-KKR) CPA (Refs. 4 and 5) has been applied, and transport properties calculated from first principles.<sup>8-10</sup> In particular, Butler and Stocks<sup>9</sup> have been able to overcome the so-called Mott  $sd$  model<sup>11</sup> in explaining the residual resistivity and the thermopower anomalies (as a function of the concentration) of such system, and that was certainly a remarkable success of the multiple scattering theory of alloys.

Recently,<sup>12</sup> we have discussed the role of the electronic topological transitions (ETT's), occurring in several metallic binary alloys when the number of valence electrons, or more generally, the electron chemical potential, is changed. We argued there that the anomalies of  $\text{Ag}_c\text{Pd}_{1-c}$  residual resistivity and thermopower had to be related to such an interesting phenomenon, predicted by Lifshitz in 1960,<sup>13</sup> although, due to the substitutional disorder, rigorously one should discuss in terms of "anomalies" rather than "transitions" (see, for example, Ref. 14, hereafter referred to as Paper I). One of the purposes of this paper is to show that, in effect, the Fermi-surface topology changes quite suddenly in those concentration intervals where also the transport coefficients show anomalies. It has been demonstrated (cf. Ref. 15, and references therein) that the anomalies of such quantities are consequences of ETT's.

As has been discussed in Paper I, also certain equilibrium quantities display anomalies at the ETT's. In effect,

on varying the concentration, under the assumption (*although it is by no means necessary*) that the bands are "rigid," the electron gas chemical potential  $\mu$  can be moved until it passes through a Van Hove singularity. Then, the density of states at  $\mu$  and the electronic grand potential must have a singularity whose "special" parts, on neglecting temperature and impurity scattering effects, can be written as

$$n_1 = \alpha \Theta(\mu - \varepsilon_c)(\mu - \varepsilon_c)^{1/2} \quad (1)$$

and

$$\Omega_1 = -\frac{4\alpha}{15} \Theta(\mu - \varepsilon_c)(\mu - \varepsilon_c)^{5/2}, \quad (2)$$

respectively. The implications of this fact are deep and, at present, not completely explored. For instance, it does not only mean that equilibrium properties like specific heat or enthalpy of mixing, etc., are affected by the ETT, but also that electronic total-energy calculations require great care in the proximity of such transitions. Disorder scattering notwithstanding, for an alloy concentration close to the "critical concentration" several spurious effects can happen, such as, for instance: (i) an ETT can occur on varying the volume, then, due to Eq. (2), the electronic total energy is not necessarily parabolic, as a function of the lattice parameter, in the neighborhood of its minimum; (ii) numerical instabilities are to be expected for solving the Kohn-Sham equations,<sup>16</sup> because the bands move across the Fermi level, thus including or excluding the singular contribution  $n_1$  to the eigenvalue sum.

We also remark that the coefficient  $\alpha$ , related to the effective-mass tensor<sup>14,17</sup> in the expression for the singularity of the density of states, can be evaluated only numerically and therefore the "size" of the effect can be estimated only after the calculation. In this context, the knowledge of the Fermi surface becomes crucial, because,

from its topological modifications, one can predict at what concentrations anomalies of the physical quantities are to be expected, although little can be said about the chance of finding an experimentally detectable effect. One of the purposes of this paper is to show that these anomalies do exist and it is just a matter of hard work to take them out. This, of course, implies an accurate analysis of the conventional definition of the Fermi surface in a disordered system, and the reader is referred to Ref. 12 and to Sec. I for such a discussion.

The question as to why silver-palladium is an important system in which to study the ETT's arises spontaneously. Opposite to other alloys, like the system Zr-Nb-Mo-Re, where the ETT's show up in a quite spectacular fashion (cf. Ref. 12, and references therein),  $\text{Ag}_c\text{Pd}_{1-c}$  is by no means a "rigid band" alloy and one could think that the application to this alloy of the above argument, based on the Van Hove singularities, is questionable, notwithstanding what is claimed in Paper I. However, owing to the fact that, for pure Pd, the Fermi level lies within the  $d$  bands while, for pure Ag, it lies in the  $sp$  bands, the pure system Fermi surfaces are greatly different in shape. In fact, the Pd Fermi surface consists in an octahedron centered at  $\Gamma$  and two hole regions: an ellipsoid centered at  $X$ , and a jungle-gym structure connecting, through  $L$ , different Brillouin zones. The Ag Fermi surface is noble-metal-like, with a  $\Gamma$  centered octahedron broken by necks at the  $L$  points, giving the typical structure of the holes. There is no doubt, then, that on increasing Ag concentration the Fermi surface shall change its connectivity, either suddenly or continuously. The corresponding ETT's will be related to such topological changes, and an interesting matter of study, in itself, is to understand how a "split band" alloy Fermi surface changes by filling the  $d$  states. An aim of this paper is to show that the  $\text{Ag}_c\text{Pd}_{1-c}$  Fermi surface also shows up sharp ETT's on increasing the  $e/a$  ratio.

Another point of interest is that a study of  $\text{Ag}_c\text{Pd}_{1-c}$  Fermi surfaces should be based on a relativistic calculation, as far as ETT's are concerned. In a nonrelativistic treatment, the single point group symmetry requires that the eigenvalues along the  $\Gamma$ - $X$  line are degenerate. That implies that the above hole structures must have a contact point along this direction. Thus they must disappear simultaneously when, on increasing the Ag concentration, the Fermi level crosses the top of the corresponding bands at the  $X$  point. Nevertheless, the spin-orbit interaction, though small, as in the present case, removes such a degeneracy.<sup>18</sup> As a consequence, the two hole pockets must close at different concentrations, in a relativistic treatment. Therefore we claim that the spin-orbit interaction is qualitatively responsible for having a concentration interval where the  $\text{Ag}_c\text{Pd}_{1-c}$  Fermi surfaces have one  $X$  pocket only. That has other qualitative consequences, as discussed above, because of the singularities in the density of states and in the electronic grand potential.

This paper is organized as follows: in Sec. II we discuss critically the definition of Fermi surface in a random alloy and present our calculation scheme. In Sec. III we present and discuss our results for  $\text{Ag}_c\text{Pd}_{1-c}$  Fermi sur-

faces and argue that a similar study is useful for  $\text{Cu}_c\text{Pt}_{1-c}$ .

## II. CALCULATION OF FERMI SURFACES IN RANDOM ALLOYS

First, it is worthwhile to establish the concept of Fermi surfaces in a random alloy. The appropriate tool for this definition is the so-called Bloch spectral function (BSF),<sup>19</sup>  $A_B(\epsilon, \mathbf{k})$ , namely, the density of states at a given  $\mathbf{k}$  point of the reciprocal space. Such a function consists, for an ideal system, in a sum of  $\delta$  functions, either as a function of the energy [when  $\epsilon$  is identical to the eigenvalue  $\epsilon_v(\mathbf{k})$ ] at fixed  $\mathbf{k}$ , or as a function of the  $\mathbf{k}$  point [when  $\mathbf{k}$  is identical to  $\mathbf{k}_v(\epsilon)$ ] at fixed  $\epsilon$ . This can be written as

$$A_B(\epsilon, \mathbf{k}) = \sum_v \delta(\epsilon - \epsilon_v(\mathbf{k})) \\ = -\frac{1}{\pi} \text{Im} \lim_{\eta \rightarrow 0^+} \sum_v \frac{1}{\epsilon - \epsilon_v(\mathbf{k}) + i\eta} \quad (3)$$

at fixed  $\mathbf{k}$  and

$$A_B(\epsilon, \mathbf{k}) = \sum_v \delta(k_\zeta - k_{\zeta v}(\epsilon)) \\ = -\frac{1}{\pi} \text{Im} \lim_{\xi \rightarrow 0^+} \sum_v \frac{C_{\zeta v}}{k_\zeta - k_{\zeta v}(\epsilon) + i\xi} \quad (4)$$

at fixed  $\epsilon$  and  $\mathbf{k}$  taken along a direction labeled  $\zeta$ . Such equations have relevance in KKR band structure method<sup>20,21</sup> and are referred to as constant  $\mathbf{k}$  [Eq. (3)] or constant energy [Eq. (4)] search.

The Fermi surface is then defined as the locus of the discontinuities of the BSF at fixed  $\epsilon = \epsilon_F$ , according to either Eq. (3) or Eq. (4). In the case of a random alloy, one may think to perform the configuration ensemble average (e.g., by means of CPA) of the eigenvalues spectrum. This shall result in the fact that the BSF will be nonzero for arbitrary values of  $\epsilon$  and  $\mathbf{k}$ , or, equivalently, in the fact that the  $\delta$  functions will broaden up in a series of Lorentzian-like peaks, i.e., in a "complex" band structure. It turns out that the former definition of Fermi surface can be extended to a random alloy, although, as an effect of disorder, one has to take care of the nonzero width of the peaks. Those make the Fermi surface "astigmatic," more or less as a defocused picture. Such an  $\epsilon$ - and  $\mathbf{k}$ -dependent broadening is equivalent to a high effective temperature. This is so high as to prevent the detection of cyclotronic resonances in a de Haas-van Alphen experiment, at least at the laboratory magnetic fields.<sup>22</sup> That notwithstanding, such a broadening might be small when compared with the Brillouin zone size, restoring robustness to our definition,<sup>12</sup> particularly if one considers the two-dimensional angular correlation of annihilation radiation (ACAR) experiments in random alloys (see, for example, Ref. 23), which prove the Fermi surface existence. Therefore one can define the Fermi surface as the locus of the peaks of the Bloch spectral function, the *average* spectrum, at fixed  $\epsilon = \epsilon_F$ .

Alternatively,<sup>19</sup> and more conveniently for actual calculations, the BSF may be defined as the imaginary part of the lattice Fourier transform of the "coherent" Green's function. This can be written as

$$A_B(\varepsilon, \mathbf{k}) = -\frac{1}{\pi} \text{Im} G^c(\varepsilon, \mathbf{k}). \quad (5)$$

In the present paper, the BSF is evaluated numerically through Eq. (5) (Refs. 12 and 19) in the KKR-CPA framework from *ab initio*, local density approximation (LDA) KKR-CPA potentials for the translationally invariant CPA “coherent” medium.<sup>24</sup>

The CPA is an elegant and accurate way of averaging the spectral properties, but it is a mean-field theory. The consequent neglect of charge fluctuations leads to an underestimation of the Madelung terms in the electronic total energy, as pointed out by several authors.<sup>25,26</sup> In order to overcome this hurdle, one might think of giving up the mean-field theory, by constructing a special quasirandom structure (SQS), which keeps the most important correlations<sup>27</sup> of the real system. However, having necessarily a different translational symmetry, it becomes difficult to study the spectral properties of the alloy; in fact, at present, no Fermi-surface calculation has appeared yet. As an alternative, if the investigation of the Fermi surface is the problem at hand, one might follow the suggestion of Johnson and Pinski,<sup>26</sup> and/or Abrikosov *et al.*,<sup>28</sup> still within the CPA framework.

Such approaches are based on the fact that the screening length of an impurity is comparable with the nearest-neighbor distance<sup>29,30</sup> in a metal and therefore one could limit the inclusion of charge fluctuations within the first shell of neighbors only. The Johnson and Pinski approach, the charge correlated CPA (cc-CPA), is equivalent to a conventional CPA calculation but with a number of components equal to twice (for a binary alloy) the number of nearest neighbors and is therefore computationally demanding; the approach of Abrikosov *et al.*, the screened CPA, is computationally faster and reduces (a factor 2 apart) to the “mean-field” solution of the cc-CPA, i.e., the excess charge on the central site is supposed to be distributed uniformly in the nearest-neighbors shell, and the Madelung energy is calculated accordingly as

$$\Delta E^{\text{scr}} = -\frac{e^2}{R_s} [c_A (\Delta Q_A)^2 + c_B (\Delta Q_B)^2], \quad (6)$$

where  $R_s$  is the nearest-neighbor distance. Recently, real-space large cell calculations (the LSMS of Nicholson *et al.*<sup>31</sup>) confirm the general prediction by Lu, Wei, and Zunger<sup>32</sup> and Johnson and Pinski<sup>26</sup> that the excess charge in a site increases linearly with the number of unlike neighbors.

Excess charge fluctuations are related to the microscopic interpretation of the Hume-Rothery factors in alloying:<sup>33</sup> size,  $e/a$  ratio, and electronegativity.<sup>34</sup> The development of the above “beyond CPA” theories is, therefore, mostly important in the context of metallic alloys theory. However, in the present case of  $\text{Ag}_c\text{Pd}_{1-c}$ , it does not appear exceedingly relevant, because the charge transfers are small and the “sizes” (equilibrium volumes) of the pure constituents are very close. Owing to these facts, the CPA approach is supposed to work as well as other more complicated and accurate schemes. In fact, as shown in Paper I, the total energies found by this

method are not very different from those of Lu, Wei, and Zunger.<sup>32</sup> The results we are going to present in the following were, then, obtained by evaluating the mean-field solution of the cc-CPA approach, applied to site potentials in the muffin-tin form.

The mathematical structure of Eq. (4) and our definition of the Fermi surface allow us to decompose the BSF, according to<sup>12</sup>

$$A_B(\varepsilon_F, k_\zeta) = \sum_{\nu=1}^{\nu_{\text{max}}} \frac{c_{\xi_\nu}(\varepsilon_F)}{[k_\zeta - k_{\xi_\nu}(\varepsilon_F)]^2 + \xi_{\xi_\nu}^2(\varepsilon_F)} \quad (7)$$

where  $k_{\xi_\nu}(\varepsilon_F)$  has the meaning of intersection of the  $\nu$ th sheet of the Fermi surface with the direction  $\zeta$  and  $\xi_{\xi_\nu}(\varepsilon_F)$  is its “astigmatism” along the same direction. The quantity  $\hbar/\xi_{\xi_\nu}$  has the meaning of “coherence length” of an electron whose momentum projection along  $\zeta$  is  $k_{\xi_\nu}(\varepsilon_F)$ , i.e., the Fermi wave vector. Then Eq. (7) can be used as a basis for a nonlinear least-square fit, in order to find the whole Fermi surface on varying directions  $\zeta$ . We remark that Eq. (7) transforms the study of the Fermi surface into the study of the constant energy BSF and therefore the study of how the BSF changes along relevant directions in the reciprocal space is equivalent to the study of the ETT’s in a random alloy.

An interesting point is that the above procedure can be applied to pure metals as well, with the prescription, based on Eq. (3), of imposing a small imaginary part to the energy. Such a trick will broaden the  $\delta$  functions a little and allows us to find the Fermi surface numerically. Repeating the same procedure for all the points of a given energy grid, also allows us to calculate the full band structure, as in a constant energy search.

### III. THE FERMI SURFACES OF $\text{Ag}_c\text{Pd}_{1-c}$

We have calculated, within the above relativistic LDA-KKR-CPA framework, in connection with the mean-field cc-CPA treatment of the charge correlations, the equilibrium lattice parameters, the SCF site potentials, and the Fermi levels for the following concentrations of silver: 0, 0.10, 0.20, 0.30, 0.35, 0.40, 0.50, 0.60, 0.70, 0.80, and 1. Our electronic total-energy calculation agrees well with the experiment and with the full-potential linear augmented plane wave SQS results of Lu, Wei, and Zunger<sup>32</sup> for the  $c=0.50$  alloy, as shown in Paper I.

The constant energy search designed by Eq. (7) has allowed us to draw the band structure of palladium that is displayed in Fig. 1. In order to broaden the  $\delta$  functions, we added a small imaginary part to the energy (0.001 Ry) and the bands were drawn by plotting the Lorentzian peak positions. As one can see, the Fermi level intersects several bands. Those relevant to the study of the ETT’s are the Van Hove singularities at the  $L$  and  $X$  points. Moreover, as we shall see, there is another saddle point at about  $\mathbf{q}_s = (0.39, 0.39, 0.47)$ . In particular, the reader can see at a glance that along the  $\Gamma$ - $X$  direction there are three interactions, namely, an  $sp$  band and two  $d$  bands. They constitute the electron pocket centered at  $\Gamma$  and two hole structures, the ellipsoid centered at  $X$  and the

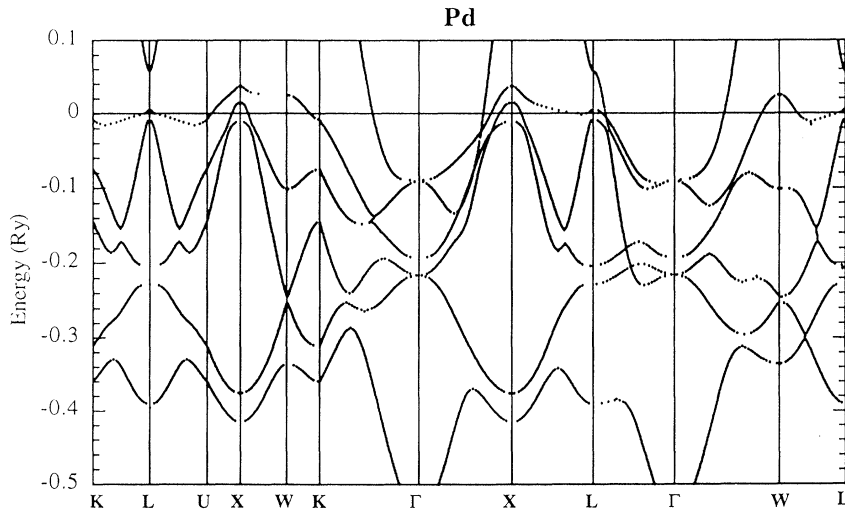


FIG. 1. The constant energy search for the band structure of palladium, along the indicated symmetry directions. The energy, relative to the Fermi level, is in rydbergs. In order to set up the Lorentzian fit procedure an imaginary part of 0.001 Ry has been added to the energy. Notice that, when the bands are flat, the constant energy fit becomes critical, either finding few spurious points or missing some point of very flat bands.

jungle-gym, as the reader can also see by inspection of Fig. 2(a). This picture shows the Fermi-surface intersection with the plane  $\Gamma K L U X$  in the reciprocal space. On increasing the  $e/a$  ratio, i.e., adding Ag impurities, such holes will get filled, and two different ETT's are to be expected at two different values of the  $e/a$  ratio, corresponding to the Fermi level passing through the spin-orbit split Van Hove singularities at  $X$  (see Fig. 1). Figure 2(b) shows our scalar relativistic calculation for the Pd Fermi surface, and one immediately realizes that such a calculation can only find, when raising the Fermi level, that the disappearance of the two hole structures must occur at the *same*  $e/a$  value, due to the degeneracy of the Van Hove singularities at  $X$ . This is a consequence of the single point group symmetry, which requires the  $d$  bands to be degenerate along the  $\Delta$  direction. The spin-orbit interaction, although small, removes such a degeneracy and compels us to proceed in our study by a fully relativistic treatment. The Pd Fermi surface of Fig. 2(a) is similar to that of Ref. 18, although we find a jungle-gym structure of the hole pockets which, opposite to Ref. 18, are connected at the  $L$  points.

Constant energy search gives us the chance to guess at which concentration intervals the ETT's should be searched for. Figure 3 clarifies what we call the "rigid band" prediction. We plot there the BSF calculated for pure Pd at different energies above the Fermi level and along the  $\Delta$  line. The peak positions describe, in the  $\epsilon$  versus  $\mathbf{k}$  plane, the dispersion of those bands. It is worth remarking here that the broadenings of the BSF peaks, along a direction, are not expected to be uniform and symmetric for a "complex" band structure. In effect, they depend upon the angle between the "band" and the constant energy surface on study (namely, flat bands look broader than nearly vertical bands) and are also affected by the Lorentzian tails of "states" close in energy.<sup>12</sup> This fact (see also the caption of Fig. 1) is the reason for a few spurious points in Fig. 1 and for the fact that few points of some very flat bands (see the band along  $XW$  at energy about 0.02) are missed. As the reader can see in Fig. 3, the three pure Pd peaks reduce at first to two then

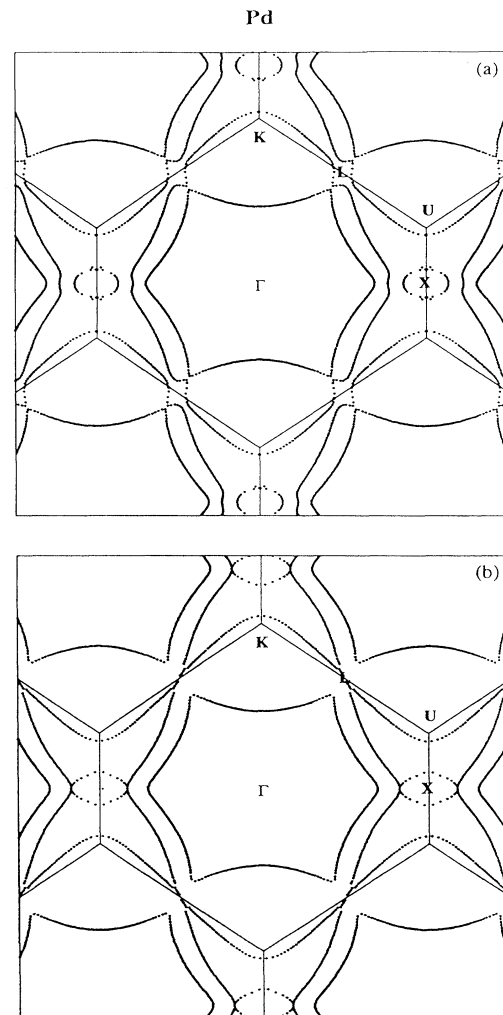


FIG. 2. The relativistic (a) and semirelativistic (b) calculation of pure Pd Fermi-surface intersections with the plane  $\Gamma K L U X$ . Notice in (b) that along the line  $\Gamma$ - $X$  the two  $X$  centered hole pockets are touching because of single point group symmetry reasons.

only to one, as the third and second peaks move out of the Brillouin zone edge. In the same picture we score for each BSF, together with the energy value relative to the Fermi level, the corresponding value of the valence electron number, as obtained by integrating the density of states. We then gain the information that the Fermi level should pass through the Van Hove singularities at  $X$  at the concentration values of about 0.35 and 0.53. Interestingly, as we will show in the following, these predictions are not surprisingly accurate, notwithstanding this alloy is not at all a rigid band system.

In Fig. 1 the reader can notice a  $d$  band that along the  $L$ - $X$  line is very flat and nearly tangent to the Fermi level. Along the same line it has two maxima, at  $L$  and  $X$ , and a minimum in between close to  $L$ . This is clearly shown in Fig. 4(a), where we plot the BSF, calculated at various energy values in a neighborhood of the Fermi level. In this picture, on the left side, the distance between  $X$  and the position of the first sharp peak measures the radius of the  $X$  centered hole ellipsoid. More relevant to our discussion is the right part of the picture, where, for energies greater than  $\epsilon_F$ , there are two broad peaks (the band is very flat) which, on lowering the energy, merge at about the Fermi level and then disappear. By drawing in Fig. 2(a) a straight line from  $L$  to  $X$ , the reader can see that such line is peeling the Fermi surface. Thus, for  $e/a < 10$ ,

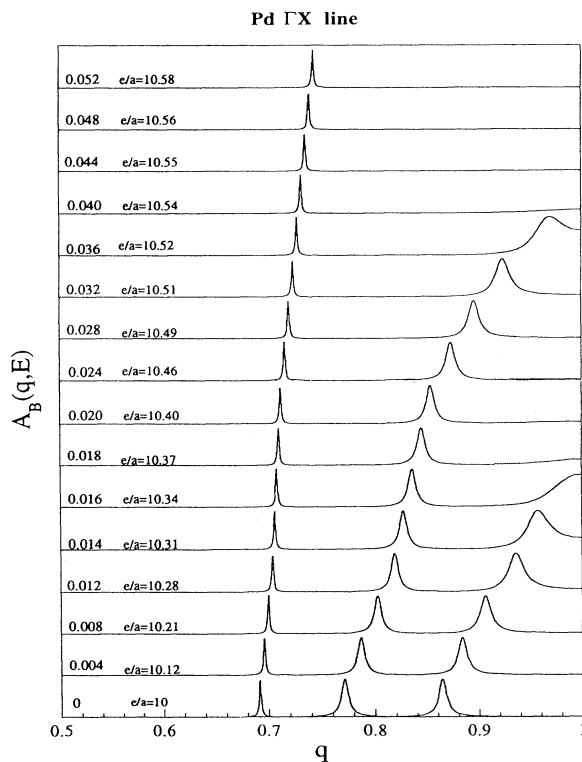


FIG. 3. The “rigid band” predictions for the disappearance of the  $X$  pockets. The BSF calculated along the  $\Gamma$ - $X$  direction, for several values of the energy distance from the Fermi level. The energy distances, in rydbergs, are indicated on the left, together with the corresponding number of valence electron per atom ( $e/a$ ).

the volume of the occupied states is such that no intersection of the band is found along the  $L$ - $X$  line, while for  $e/a > 10$  two intersections are found. This is the evidence of a connectivity change in the Fermi surface, which, however, is not necessarily along the  $L$ - $X$  line. By looking at Fig. 2(a), we observe that the Pd jungle-gym structure has its smallest section along a direction  $\Gamma$  (0.47,0.47,0.56). Therefore, we plot in Fig. 4(b) the BSF along this line, in a fine energy grid. There one can see two peaks, which merge at higher energies, thus showing that the jungle-gym connection disrupts at  $q_s \approx (0.39, 0.39, 0.47)$ , leaving two hole pockets, a little hole one centered at  $L$  and another one centered at  $X$ . Moreover, the band described by the peak positions shows clearly a maximum at  $q_s$ , while along  $L$ - $X$  we found a minimum. This establishes that  $q_s$  is a saddle point. The corresponding ETT occurs at an Ag concentration that the rigid band model estimates to be between 0.05 and 0.08. However, a more accurate estimate of the critical concentration is particularly difficult, since in the present case the band involved is very flat and very sensitive to the introduction of a small inverse lifetime. Thus the alloying with a small amount of Ag would not allow a

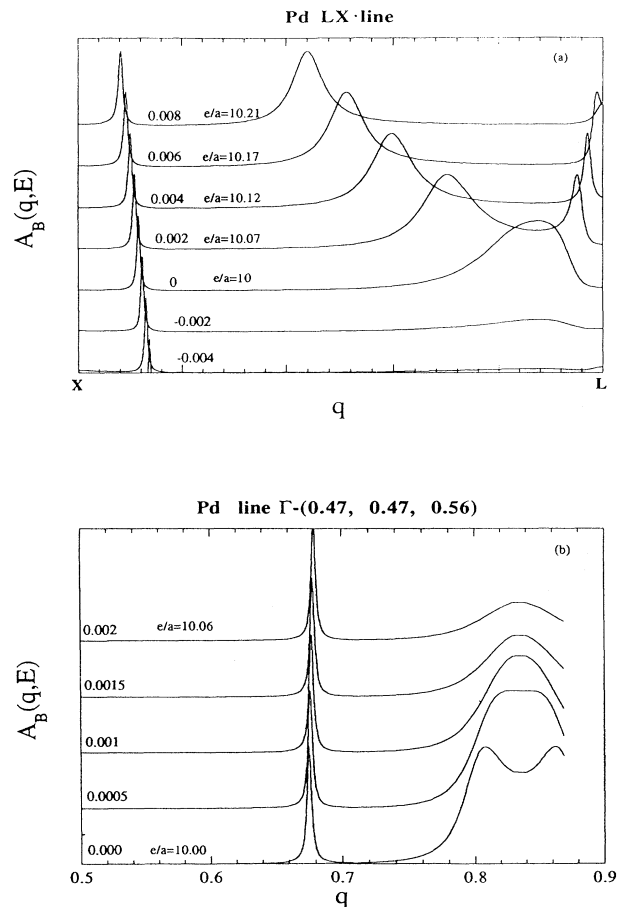


FIG. 4. The BSF along the  $L$ - $X$  line (a) and along the line  $\Gamma$ (0.47,0.47,0.56). (b) The notation is the same as Fig. 3. The saddle point, corresponding to the broad maximum in (b), is  $q_s \approx (0.39, 0.39, 0.47)$ .

reliable resolution of the relevant state. On the other hand, the rigid band model is expected to be reasonably accurate in such a narrow concentration range.

In Fig. 5 the reader can see the DOS's for all the alloys studied. The Fermi level moves from the  $d$  towards the  $sp$  states as the Ag concentration increases. The reader can notice the presence of the so-called virtual bound states, the primary feature of split band alloys. The disorder smears out the sharpest features in the DOS as the concentration approaches intermediate values. The DOS's shown appear to be consistent with the nonrelativistic calculations of Winter and Stocks.<sup>4</sup>

Having gained confidence in our constant energy search, we can activate our "rigid band" machine again for the concentration  $c=0.20$  and  $c=0.50$ . We notice also that the rigid band model is supposed to work well in small concentration intervals. The results, to be compared with Fig. 3, are shown in Figs. 6 and 7, respectively. By comparisons with Fig. 3 one immediately sees the large (as it must be for a split band alloy) effect of the disorder, in the sense that the peaks become broad ( $c=0.20$ ) and very broad ( $c=0.50$ ). However, they still have a dispersion and move out of the Brillouin zone and that happens at concentration values very close to the ones predicted above, by starting from pure palladium. The explanation of this surprising result is based on the fact that the system is a split band alloy. In fact, the Ag-like  $d$  states are placed at high binding energies, while,

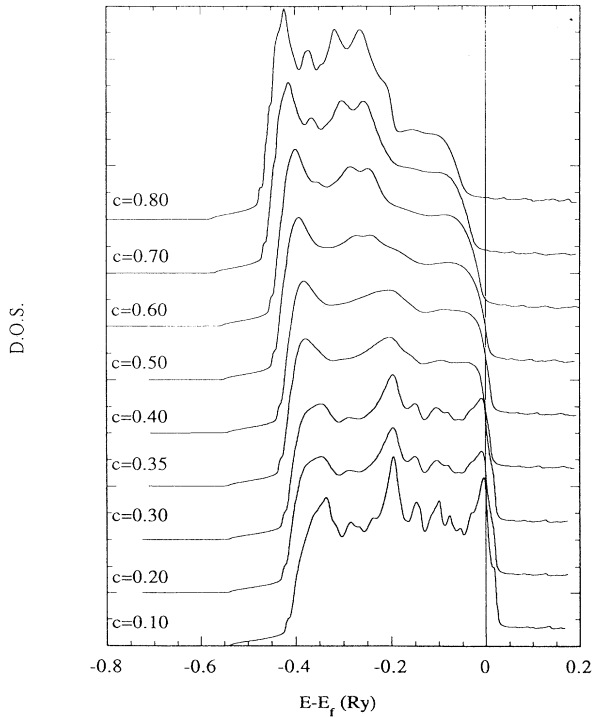


FIG. 5. The  $\text{Ag}_c\text{Pd}_{1-c}$  total densities of states for the indicated concentrations, ranging from  $c=0.10$  to  $c=0.80$ , as calculated by relativistic LDA-KKR-CPA. The energy, in rydbergs, is relative to the Fermi level. Notice the classical split band behavior as Ag content is increased, and that the Fermi level moves away from the  $d$  states.

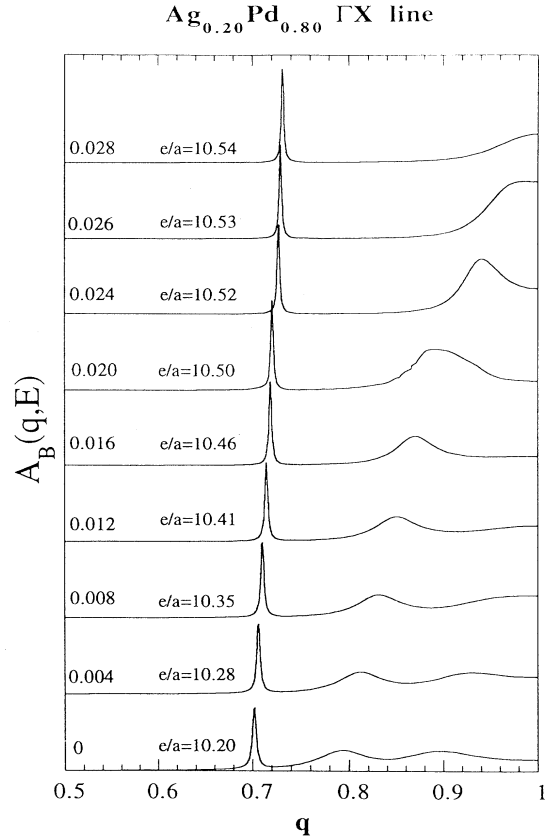


FIG. 6. The same rigid band predictions as in Fig. 3 but starting from  $\text{Ag}_{0.20}\text{Pd}_{0.80}$ . Notice (see also the text) that the predictions for the "critical concentrations" are very close to that of Fig. 3.

the states near the Fermi level are mostly Pd like. The hybridization with Ag states does not affect their positions but essentially only their width. Figure 8 shows the prediction that the neck should open up just below  $c=0.70$ , activating the rigid band procedure from  $c=0.70$ .

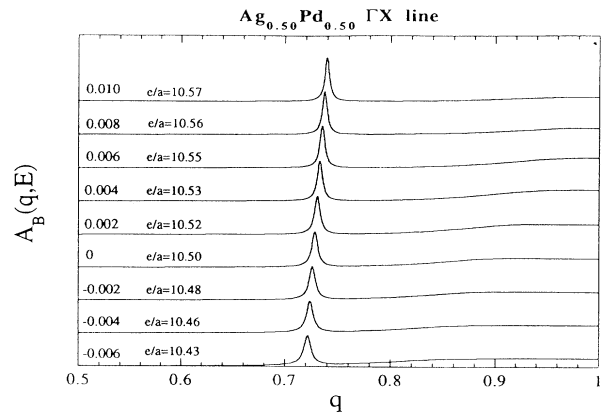


FIG. 7. The same rigid band predictions as in Figs. 3 and 6 but starting from  $\text{Ag}_{0.50}\text{Pd}_{0.50}$ , and only for the prediction of the closure of the second hole pocket at  $X$ . Notice (see also the text) that the prediction for the "critical concentration" is very close to those of Figs. 3 and 6.

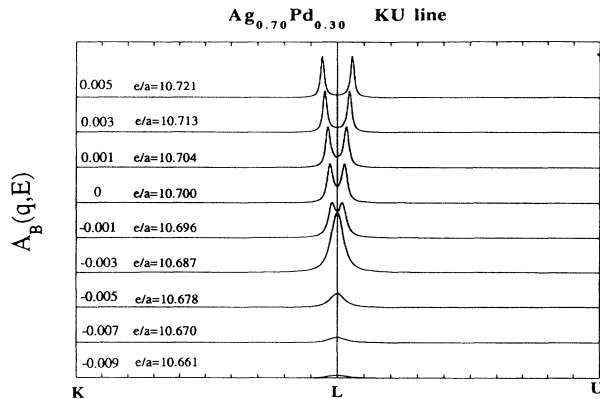


FIG. 8. The rigid band prediction for the neck opening, around  $c = 0.70$ . The notation is identical to that of Fig. 3.

In Figs. 9(a)–9(d) we show the Fermi-surface intersections with the plane (110) for the indicated concentrations. One can see in more detail how the necks open up just below  $c = 0.70$ . Unfortunately, analogous pictures for the Pd-rich alloys are not very illustrative, because the disorder affects largely the BSF's, as shown in Figs. 6 and 7, making our fitting procedures less reliable. What is completely clear [see Fig. 9(d)], however, is that around  $c = 0.60$  the second  $X$  pocket has already disappeared while the neck is not open yet. Our calculation, then, predicts that there is a fairly large concentration interval where the Fermi surface is simply connected as for a simple metal, although its shape is by no means spherical.

In order to gain a better understanding of the Fermi-surface connectivity variations, particularly at a low content of Ag, we display in Fig. 10 the BSF's calculated along the meaningful Brillouin zone edges, on varying the

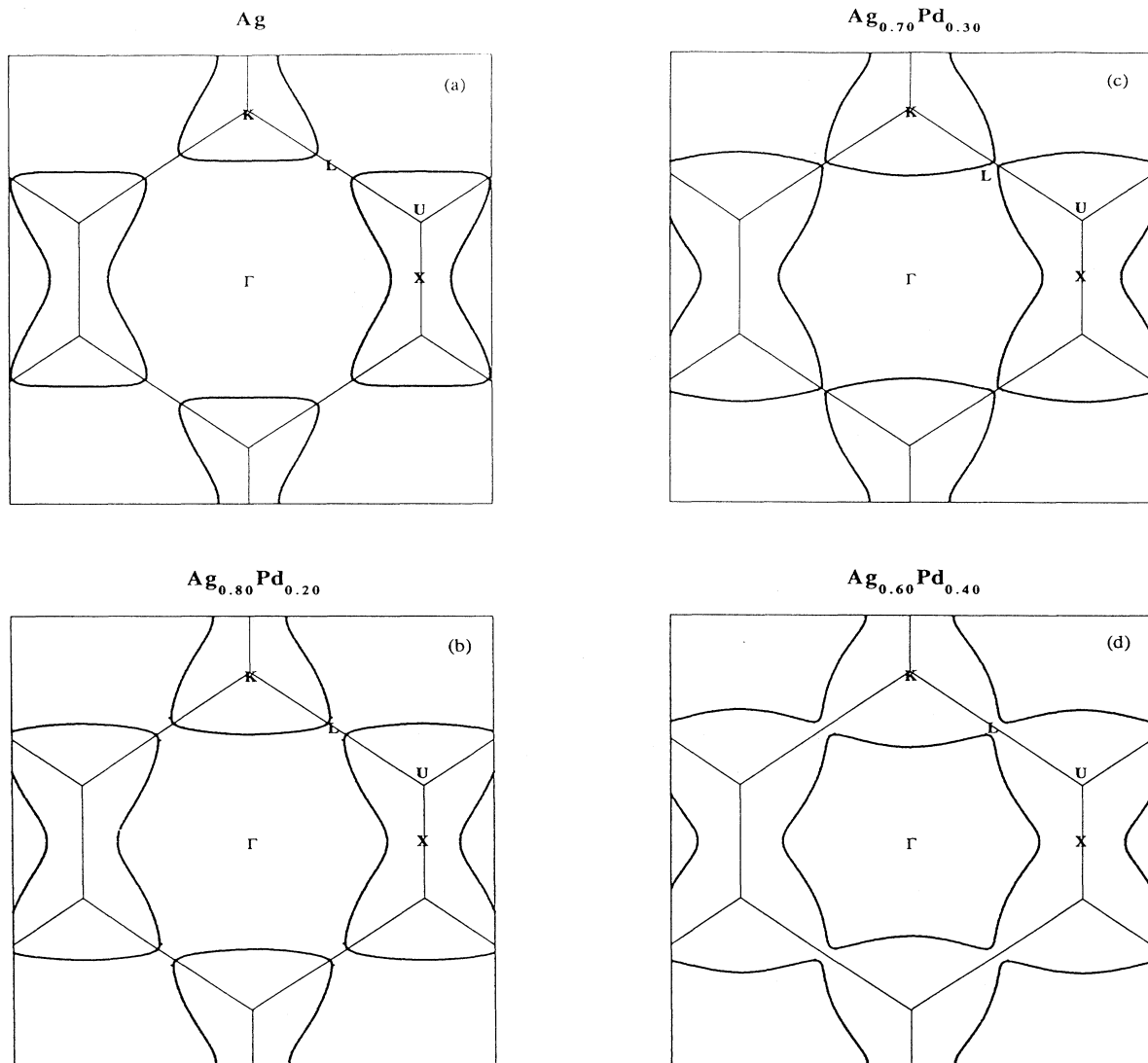


FIG. 9. The Fermi-surface intersections with the  $\Gamma KLUX$  plane for pure Ag (a),  $\text{Ag}_{0.80}\text{Pd}_{0.20}$  (b),  $\text{Ag}_{0.70}\text{Pd}_{0.30}$  (c),  $\text{Ag}_{0.60}\text{Pd}_{0.40}$  (d). Notice how the neck radii along  $KL$  reduce while approaching the critical concentration  $c = 0.70$ . The  $c = 0.60$  alloy is in the “simple metal” region (see text).

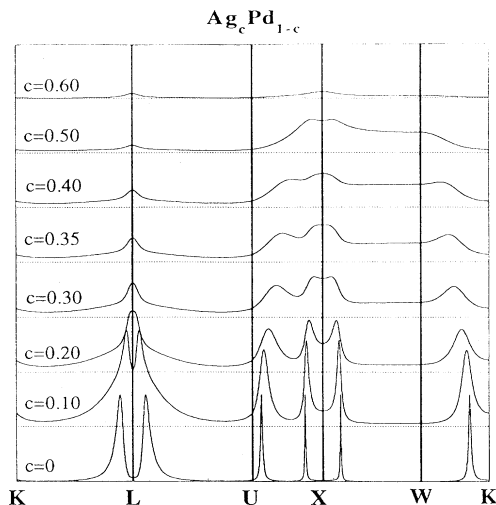


FIG. 10. The BSF calculated along the Brillouin zone boundaries, as indicated, for the concentration ranging from  $c=0$  to  $c=0.60$ . In order to make it plottable in the same picture, the BSF for pure Pd has been reduced by a scale factor. Notice the virtually complete absence of states in the case  $c=0.60$ , and how the peaks collapse and smoothly disappear as passing through the critical concentrations.

concentration. There is no rigid band assumption at this time. One can see there that, the disorder notwithstanding a lot of action takes place. At first, around  $c=0.20$  the pocket at  $L$ , left after the small neck disruption at  $c=0.07$ , “smoothly” disappears. Then, the ellipsoid pocket closes at  $X$  around  $c=0.35$ . Smoothly again, the second  $X$  pocket disappears just above  $c=0.50$ . In Fig. 11 the neck opening is then displayed, and that appears as an abrupt disruption around  $c=0.70$ . It is worth remarking here that such ETT’s occur at the same concentration values where also the calculated lattice parameter deviates from Vegard’s law, as shown in Paper I.

Figures 10 and 11 tell us a lot about ETT’s in random alloys. We see that the disorder can make the Fermi surface modifications versus concentration hard to follow, and, perhaps, can make questionable the meaning of the Fermi surface itself. In fact, in the alloys studied, the  $X$  pocket and the jungle gym structure are more “defocused” than the central octahedron. Moreover, one may think that, at the concentrations where the connectivity changes are sudden, the anomalies in, say, transport coefficients should be more pronounced. However, it is not so. The “weight” of an ETT is related to the effective mass tensor at the Van Hove singularity, therefore what could seem a continuous change in connectivity, because it involves a broad band, could show up in a sharp fashion in some physical property. In effect, by looking at the experimental diffusion thermopower of this alloy,<sup>6</sup> one can see a growth in the region  $0 \leq c \leq 0.10$  and a broad plateau in the region  $0.10 \leq c \leq 0.40$ , where we find two changes in connectivity; a sharp peak around 0.50, where a smooth disappearance of the  $X$  pocket occurs, a rapid decrease, then a variation of slope around  $c=0.70$ , where suddenly the neck appears. Therefore we

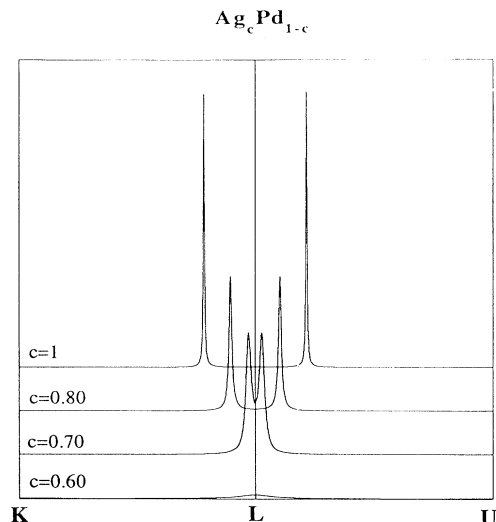


FIG. 11. The BSF along the line  $KLU$ , for the concentration indicated. Notice the neck disruption as the Pd content increases.

claim, as claimed by Butler and Stocks<sup>9</sup> and theoretically demonstrated by Varlamov, Egorov, and Pantsulaya,<sup>15</sup> that the changes in connectivity we found in  $Ag_cPd_{1-c}$ , on increasing Ag atomic concentration, have relevant consequences on physical properties (see Paper I) of these metals.

We notice also that in  $Cu_cPt_{1-c}$ , apparently similar to  $Ag_cPd_{1-c}$  because isoelectronic, the “simple metal” region does not exist, as preliminary calculations show.<sup>35</sup> In that system, as discussed by Clark *et al.*,<sup>36</sup> the neck at  $L$  opens up at a much lower concentration and, in effect, the authors claim that the *contemporary* existence of Van Hove singularities at  $L$  and  $X$  is the cause of the  $L_1$  ordering of that system. In Ref. 32, the authors claim that also  $Ag_{0.50}Pd_{0.50}$  could order, at low temperature, into the  $L_1$  structure. Unfortunately, the low-temperature phase diagram of this system, notwithstanding it is one of the most studied alloy, is not known.<sup>37</sup> Our total-energy calculation predicts (see Paper I) also that the random phase is more stable than the segregated one, and that means that an ordered phase must exist. However, on the grounds of our Fermi-surface study, we can say that, because of the fact that the  $X$  pocket closes, on increasing Ag content, at a concentration value of about 0.53 and the neck opens at about 0.70, if the AgPd compound had the  $L_1$  structure, the mechanism of such order-disorder transition must be different from and “weaker” than that proposed for CuPt.

#### IV. CONCLUSIONS

We have studied by relativistic KKR-CPA the Bloch spectral functions of  $Ag_cPd_{1-c}$  at the Fermi levels of these alloys. We have found that, on varying the Ag concentration, five changes in the Fermi-surface topology occur near the concentration values  $c=0.06$  (a neck dis-



ruption),  $c=0.20$  (disappearance of a hole pocket centered at  $L$ ),  $c=0.35$  (disappearance of the first hole pocket centered at  $X$ ),  $c=0.53$  (disappearance of the second hole pocket centered at  $X$ ), and  $c=0.70$  (neck opening at  $L$ ). As claimed in Paper I, irrespective of the fact that the rigid band model does not apply, equilibrium and transport properties of such metallic alloys must show anomalies around the quoted concentration values. Moreover, the "transition" taking place at  $c=0.35$  cannot be detected by a nonrelativistic treatment, on symmetry grounds, and in the concentration region between 0.55 to 0.69 the Fermi surface of these alloys is, although not at all spherical, simply connected as in a simple metal.

Our study also suggests that the ETT's in alloys between noble metals and Pd or Pt, can occur at very different critical concentrations. In particular, the succession in which the neck at  $L$  opens and the hole pockets at  $X$  close as the  $e/a$  ratio increases, seems to be relevant for the ordering mechanism of these alloys. We also pointed out the qualitative importance of the spin-orbit

interaction in establishing the Fermi-surface topologies. These evidences suggest the utility of a systematic study of the Fermi surfaces of the above systems, where, together with many other effects, the spin-orbit interaction changes considerably with the atomic species and with their concentrations. Work is in progress on this line.

#### ACKNOWLEDGMENTS

We gratefully acknowledge enlightening discussions with J. S. Faulkner, G. M. Stocks, J. B. Staunton, and A. A. Varlamov. This work has been sponsored by Istituto Nazionale di Struttura della Materia (INFM) and Ministero per l'Università e Ricerca Scientifica (MURST). We also acknowledge the support of Centro di Calcolo dell'Università di Messina and the use of the IBM R550/6000 mod.580 cluster, by PVM, where the calculations have been performed. At last, but not least, we acknowledge the opportunities of meetings and discussions supported by the HCM  $\Psi_k$  network on Ab Initio (from electronic structure) Processes in Complex Materials.

- 
- <sup>1</sup>N. F. Mott and H. Jones, *The Theory of the Properties of Metals and Alloys* (Oxford University Press, Oxford, 1936).
- <sup>2</sup>G. M. Stocks, R. H. Williams, and J. S. Faulkner, *J. Phys. F* **3**, 1688 (1973).
- <sup>3</sup>A. J. Pindor, W. M. Temmerman, B. L. Gyorffy, and G. M. Stocks, *J. Phys. F* **10**, 2617 (1980).
- <sup>4</sup>H. Winter and G. M. Stocks, *Phys. Rev. B* **27**, 898 (1983).
- <sup>5</sup>G. M. Stocks, in *The Electronic Structure of Complex Systems*, Vol. 113 of NATO Advanced Study Institute, Series B: Physics, edited by P. Phariseau and W. M. Temmerman (Plenum, New York, 1984).
- <sup>6</sup>B. R. Coles and J. C. Taylor, *Proc. R. Soc. London Ser. A* **267**, 139 (1962).
- <sup>7</sup>A. M. Gèunault, *Philos. Mag.* **30**, 641 (1974).
- <sup>8</sup>G. M. Stocks and W. H. Butler, *Phys. Rev. Lett.* **48**, 55 (1982).
- <sup>9</sup>W. H. Butler and G. M. Stocks, *Phys. Rev. B* **29**, 4217 (1984).
- <sup>10</sup>J. C. Swihart, W. H. Butler, G. M. Stocks, D. M. C. Nicholson, and R. C. Ward, *Phys. Rev. Lett.* **57**, 1181 (1986).
- <sup>11</sup>N. F. Mott, *Proc. Phys. Soc.* **47**, 571 (1935).
- <sup>12</sup>E. Bruno, B. Ginatempo, E. S. Giuliano, A. V. Ruban, and Yu. Kh. Vekilov, *Phys. Rep.* **249**, 353 (1994).
- <sup>13</sup>I. M. Lifshitz, *Zh. Eksp. Teor. Fiz* **33**, 1569 (1960) [*Sov. Phys. JETP* **11**, 1130 (1960)].
- <sup>14</sup>E. Bruno, B. Ginatempo, and E. S. Giuliano, preceding paper, *Phys. Rev. B* **52**, 14 544 (1995).
- <sup>15</sup>A. A. Varlamov, V. S. Egorov, and A. V. Panssulaya, *Adv. Phys.* **38**, 469 (1989).
- <sup>16</sup>W. Kohn and L. J. Sham, *Phys. Rev.* **140**, A1133 (1965).
- <sup>17</sup>Ya. M. Blanter, M. I. Kaganov, A. V. Panssulaya, and A. A. Varlamov, *Phys. Rep.* **245**, 160 (1994).
- <sup>18</sup>O. K. Andersen, *Phys. Rev. B* **2**, 883 (1970).
- <sup>19</sup>J. S. Faulkner and G. M. Stocks, *Phys. Rev. B* **21**, 3222 (1980).
- <sup>20</sup>I. Korringa, *Physica* **13**, 392 (1947).
- <sup>21</sup>W. Kohn and N. Rostoker, *Phys. Rev.* **4**, 1111 (1954).
- <sup>22</sup>J. S. Faulkner and G. M. Stocks, in *Physical Phenomena at High Magnetic Fields*, edited by E. Manousakis, P. Schlottmann, P. Kumar, K. Bedell, and F. M. Mueller (Addison-Wesley, Reading, MA, 1991), p. 518.
- <sup>23</sup>S. Berkö, in *Positron Solid State Physics*, edited by W. Brandt and A. Dupasquier (North-Holland, Amsterdam, 1983).
- <sup>24</sup>D. D. Johnson, B. L. Gyorffy, D. M. Nicholson, F. J. Pinski, and G. M. Stocks, *Phys. Rev. Lett.* **56**, 2088 (1986).
- <sup>25</sup>R. Magri, S.-H. Wei, and A. Zunger, *Phys. Rev. B* **42**, 11 388 (1990).
- <sup>26</sup>D. D. Johnson and F. J. Pinski, *Phys. Rev. B* **48**, 11 553 (1993).
- <sup>27</sup>A. Zunger, S.-H. Wei, L. G. Ferreira, and J. E. Bernard, *Phys. Rev. Lett.* **65**, 353 (1990).
- <sup>28</sup>I. A. Abrikosov, Yu. H. Vekilov, P. A. Korzhavyi, A. V. Ruban, and I. E. Shilkrot, *Solid State Commun.* **83**, 867 (1992).
- <sup>29</sup>A. A. Abrikosov, *Fundamentals of the Theory of Metals* (North-Holland, Amsterdam, 1988).
- <sup>30</sup>R. Zeller, *J. Phys. F* **17**, 2123 (1987).
- <sup>31</sup>D. M. C. Nicholson, G. M. Stocks, Y. Wang, W. A. Shelton, Z. Szotek, and W. M. Temmerman, *Phys. Rev. B* **50**, 14 686 (1994).
- <sup>32</sup>Z. W. Lu, S.-H. Wei, and A. Zunger, *Phys. Rev. B* **44**, 10 470 (1991).
- <sup>33</sup>F. J. Pinski, B. Ginatempo, D. D. Johnson, J. B. Staunton, G. M. Stocks, and B. L. Gyorffy, *Phys. Rev. Lett.* **66**, 766 (1991).
- <sup>34</sup>W. Hume-Rothery and G. V. Raynor, *The Structure of Metals and Alloys*, Monograph and Report Series Vol. 13 (IOP, London, 1954).
- <sup>35</sup>E. Bruno, B. Ginatempo, and E. S. Giuliano, in *Stability of Materials*, edited by A. Gonis, P. E. A. Turchi, and J. Kudrinskij (Plenum, New York, in press).
- <sup>36</sup>J. F. Clark, F. J. Pinski, P. A. Sterne, D. D. Johnson, J. B. Staunton, and B. Ginatempo, in *Metallic Alloys: Experimental and Theoretical Perspectives*, Vol. 256 of NATO Advanced Study Institute, Series E: Applied Physics, edited by J. S. Faulkner and R. G. Jordan (Kluwer Academic, Dordrecht, 1993).
- <sup>37</sup>T. B. Massalski, *Binary Alloy Phase Diagram, Vol. 1* (ASM International, Metals Park, 1990).